NRAMP6 and NRAMP1 cooperatively regulate root growth and manganese translocation under manganese deficiency in Arabidopsis

Lun Li, Zongzheng Zhu, Yonghui Liao, Changhong Yang, Ni Fan, Jie Zhang, Naoki Yamaji, Léon Dirick, Jian Feng Ma, Catherine Curie, et al.

Ma Jian Feng (Orcid ID: 0000-0003-3411-827X)
Huang Chao-Feng (Orcid ID: 0000-0002-1486-741X)

NRAMP6 and NRAMP1 cooperatively regulate root growth and manganese translocation under manganese deficiency in *Arabidopsis*

Lun Li[1,3#], Zongzheng Zhu[1,2#], Yonghui Liao[1#], Changhong Yang[1], Ni Fan[1,2], Jie Zhang[1], Naoki Yamaji[4], Léon Dirick[5], Jian Feng Ma[4], Catherine Curie[5], and Chao-Feng Huang[1,2,3,*]

[1] Shanghai Center for Plant Stress Biology & National Key Laboratory of Plant Molecular Genetics, Center for Excellence in Molecular Plant Sciences, Chinese Academy of Sciences, Shanghai 200032, China; [2] University of the Chinese Academy of Sciences, Beijing 100049, China; [3] State Key Laboratory of Crop Genetics and Germplasm Enhancement, College of Resources and Environmental Science, Nanjing Agricultural University, Nanjing 210095, China; [4] Institute of Plant Science and Resources, Okayama University, Chuo 2-20-1, Kurashiki 710-0046, Japan; [5] IPSiM, Univ Montpellier, CNRS, INRAE, Institut Agro, Montpellier, France.

[#]These authors contributed equally to this work

*Correspondence author: Chao-Feng Huang, huangcf@cemps.ac.cn; Tel: +86-21-54924320

Running title:

NRAMP6 is required for manganese utilization

Keywords: manganese transport, NRAMP6, NRAMP1, root growth, manganese translocation, long-distance signaling, *Arabidopsis thaliana*

This article has been accepted for publication and undergone full peer review but has not been through the copyediting, typesetting, pagination and proofreading process which may lead to differences between this version and the Version of Record. Please cite this article as doi: 10.1111/tpj.15754

SUMARRY

The essential micronutrient manganese (Mn) in plants regulates multiple biological processes including photosynthesis and oxidative stress. Some Natural resistance-associated macrophage proteins (NRAMPs) have been reported to play critical roles in Mn uptake and reutilization in low Mn conditions. NRAMP6 was demonstrated to regulate cadmium tolerance and iron utilization in Arabidopsis. Nevertheless, it is unclear whether NRAMP6 plays a role in Mn nutrition. Here, we report that NRAMP6 cooperates with NRAMP1 to be involved in Mn utilization. Mutation of *NRAMP6* in *nramp1* but not wild-type (WT) background reduces root growth and Mn translocation from the roots to shoots under Mn deficient conditions. Grafting experiments revealed that *NRAMP6* expression in both the roots and shoots is required for root growth and Mn translocation under Mn deficiency. We also showed that NRAMP1 could replace NRAMP6 to sustain root growth under Mn deficiency, but not vice versa. Mn deficiency does not affect the transcript level of *NRAMP6*, but is able to increase and decrease the protein accumulation of NRAMP6 in roots and shoots, respectively. Furthermore, NRAMP6 can be localized to both the plasma membrane and endomembranes including ER, and Mn deficiency enhances the localization of NRAMP6 to the plasma membrane in Arabidopsis plants. NRAMP6 could rescue the defective growth of yeast mutant Δ*smf2* that is deficient in endomembrane Mn transport. Our results reveal the important role of NRAMP6 in Mn nutrition and in the long-distance signaling between the roots and shoots under Mn deficient conditions.

INTRODUCTION

Manganese (Mn) is an indispensable nutrient element for most organisms including plants. Mn is essentially required for photosynthesis and antioxidant defense through acting as a constituent of the oxygen-evolving complex in photosystem II (PSII) and manganese superoxide dismutase (MnSOD), respectively (Marschner, 2012). Mn can

also function as a cofactor or activator for over 30 enzymes to regulate diverse biological processes (Marschner, 2012). Mn deficiency in plants normally occurs in calcareous soils or alkaline soil with high pH, which greatly restrict the availability of Mn for plants (Schmidt et al., 2016). The typical symptoms of plant Mn deficiency include diffuse and/or interveinal chlorosis in younger leaves and reduced root and shoot growth (Marschner, 2012). Under serious Mn deficiency, root hair growth can also be inhibited (Gao et al., 2018).

Plants utilize a number of transporters to mediate Mn uptake, translocation and distribution. Natural Resistance-Associated Macrophage Proteins (NRAMPs) that act as proton/metal symporters have been reported to play crucial roles in Mn nutrition in plants. OsNRAMP5 has been shown to be essentially required for Mn uptake and translocation in rice (Sasaki *et al.*, 2012, Yang *et al.*, 2014), while OsNRAMP3 is involved in the distribution of Mn to young leaves and panicles in low Mn conditions (Yamaji et al., 2013). In *Arabidopsis*, there are six NRAMP family proteins. NRAMP1 is a plasma membrane-localized high-affinity Mn influx transporter and plays a vital role in root Mn uptake (Cailliatte et al., 2010). Mutation of *NRAMP1* reduces root and shoot growth in low Mn conditions. NRAMP3 and NRAMP4 are localized to the tonoplast and are redundantly involved in the remobilization of Mn from vacuoles to chloroplasts under Mn deficiency (Lanquar et al., 2010), although both proteins were initially documented to redundantly regulate iron (Fe) remobilization under Fe-deficient conditions (Lanquar et al., 2005). Recently, NRAMP2 was reported to be localized to the trans-Golgi network (TGN) and plays a critical role in the reutilization of Golgi Mn (Alejandro *et al.*, 2017, Gao *et al.*, 2018). Mutation of *NRAMP2* reduces root growth and leaf chlorophyll accumulation. NRAMP6 was shown to be able to transport cadmium (Cd) and Fe to modulate Cd tolerance and Fe utilization, respectively (Cailliatte *et al.*, 2009, Li *et al.*, 2019). Nevertheless, whether NRAMP6 plays a role in Mn nutrition is still unknown.

In addition to NRAMP proteins, members of other transporter families are also involved in Mn transport and utilization in low Mn conditions. The Iron Regulated Transporter 1 (IRT1), a member of ZIP family, was initially identified as a

high-affinity iron (Fe) transporter that also plays a role in Mn uptake in *Arabidopsis* in Fe deficient conditions (Korshunova *et al.*, 1999, Vert *et al.*, 2002). In rice, the MTP/CDF family member OsMTP9 is involved in both Mn uptake and translocation (Ueno et al., 2015). AtZIP1 and AtZIP2, two other ZIP members, were reported to regulate Mn translocation from roots to shoots (Milner et al., 2013). The UPF0016 family members PAM71 (PHOTOSYNTHESIS AFFECTED MUTANT71) and CMT1 (Chloroplast Manganese Transporter 1), which are localized in the thylakoid membrane and the inner chloroplast envelope, respectively, were shown to mediate the uptake of Mn to thylakoid lumen and to the chloroplast stroma (Schneider *et al.*, 2016, Eisenhut *et al.*, 2018, Zhang *et al.*, 2018). Recently, the Golgi-localized PML3 of the UPF0016 family was demonstrated to mediate Mn uptake into Golgi, which is critical for Golgi glycosylation and cell wall biosynthesis through activating Golgi-localized mannosidases or glycosyltransferases (Yang *et al.*, 2021). The Golgi-localized AtECA3, which belongs to the Ca^{2+}-ATPase subfamily of P-type ATPase superfamily, has also been reported to mediate Mn transport into Golgi for Mn utilization and plant growth under Mn deficiency (Mills et al., 2008).

In response to changing nutrient availability in soils, plants develop adaptive systemic responses and exhibit a high degree of plasticity of plant growth and development. Long-distance signaling between roots and shoots has been reported to be crucial for the adaptive responses of plants to the alterations in nutrient status (Liu *et al.*, 2009, Ko and Helariutta, 2017). For instance, nitrate influx and the expression of the high-affinity nitrate transporters-encoding genes in roots can be regulated by shoot-derived signals (Forde, 2002, Liu *et al.*, 2009). Shoot-to-root communication is also important for root growth and development under different nitrate concentrations. Cytokinins and carboxy-terminally encoded peptides (CEPs) have been demonstrated to be critical players in the shoot-to-root long distance signaling of plants in response to different nitrogen status (Tabata *et al.*, 2014, Ko and Helariutta, 2017). Shoot-to-root signaling is also critical for plants adapted to the deficiency of other macronutrients such as phosphorus and sulfur (Liu et al., 2009). In addition to the macronutrients, root acquisition of the micronutrient iron also involves long-distance

signaling, via a shoot-derived signal (Grusak and Pezeshgi, 1996, Rogers and Guerinot, 2002). Recently, a peptide family called IMA or FEP was found to be involved in such long-distance Fe signaling in plants (Grillet *et al.*, 2018, Hirayama *et al.*, 2018). Nevertheless, it is still uncertain whether Mn uptake in plants relies on shoot-to-root signaling.

In the present study, we characterized the role of NRAMP6 in Mn nutrition and found that NRAMP6 plays a cooperative role with NRAMP1 in the regulation of root growth and root-to-shoot Mn translocation under Mn deficient conditions. Interestingly, our grafting experiments showed that mutation of *NRAMP6* in shoots is required for the defective root growth and Mn translocation in *nramp6nramp1* double mutant, suggesting that NRAMP6 is involved in long-distance Mn signaling. Furthermore, we found that although mRNA expression of *NRAMP6* is not affected by Mn deficiency, its protein level and subcellular localization was altered in response to Mn deficiency, implying that *NRAMP6* is subjected to post-transcriptional regulation by Mn deficiency.

RESULTS

Knockout of *NRAMP6* in *nramp1* background reduces root growth in low Mn conditions

To determine whether NRAMP6 is involved in the regulation of Mn homeostasis in *Arabidopsis*, we used the *nramp6-1* knockout mutant previously reported (Cailliatte *et al.*, 2009, Li *et al.*, 2019). We also generated a second mutant allele of *NRAMP6*, *nramp6-2*, by the CRISPR/Cas9 technology (Ma and Liu, 2016). The *nramp6-2* mutant has a frameshift mutation (1-bp insertion located 15 bp downstream of the start codon) in the *NRAMP6* gene (Figure 1a). Both *nramp6-1* and *nramp6-2* single mutants did not show defective phenotype under Mn deficient conditions (Figure 1b). Considering the close sequence homolog between NRAMP6 and NRAMP1 in *Arabidopsis*, we asked whether both transporters were functionally cooperative by generating *nramp6-1nramp1* and *nramp6-2nramp1* double mutants. The six

genotypes showed no difference of growth in Mn replete conditions (Figure 1b and 1c). Under Mn deficient conditions, however, root growth of *nramp1* was more inhibited than that of WT as previously shown (Cailliatte et al., 2010). Interestingly, this growth defect was strongly exacerbated in the two double mutants (Figure 1b and 1c). The short-root phenotype of the double mutants was gradually rescued with the increase of Mn supply and 10 μM Mn was required to fully recover the root growth (Figure 1b and 1c), while 2 μM Mn was able to rescue the defective root growth of *nramp1* completely. In addition to increased root growth inhibition, the double mutants also showed shorter root hair than *nramp1* under Mn deficiency (Figure 1d and 1e). These results demonstrate that NRAMP6 and NRAMP1 have overlapping functions in modulating root growth and root hair elongation in low Mn conditions.

To confirm that *NRAMP6* is required for sustaining the root growth and root hair elongation in *nramp1* background under Mn deficiency, we introduced the WT *NRAMP6* gene into the *nramp6-1nramp1* double mutant. Measurement of root growth under Mn deficiency in two independent transgenic lines showed recovery up to the *nramp1* mutant level (Figure S1a and S1b). Defective root hair growth in the double mutant was also rescued in the transgenic lines under Mn deficient conditions (Figure S1c and S1d). These results indicate that the increased inhibition of root growth and root hair elongation in the double mutants compared to *nramp1* is induced by the *nramp6* mutations.

Mutation of *NRAMP2* also causes reduced root growth in low Mn conditions (Gao et al., 2018). To investigate whether NRAMP6 plays a cooperative role with NRAMP2 in the regulation of root growth, we generated *nramp6-1nramp2* double mutant to analyze the sensitivity to Mn deficiency. The result showed that Mn deficiency-induced inhibition of root growth in *nramp6-1nramp2* was similar to that in *nramp2* single mutant (Figure S2a and S2b), although both mutants displayed shorter root growth than the WT under Mn deficient conditions. Together, these results demonstrate that NRAMP6 plays a cooperative role with NRAMP1, but not with NRAMP2, to sustain root growth when Mn availability is limiting.

Mutation of *NRAMP6* affects Mn translocation from roots to shoots

To analyze the effect of the *nramp6* mutation on Mn accumulation, we firstly grew the plants of WT, *nramp1*, *nramp6-1*, *nramp6-2* and double mutants under Mn sufficient conditions and then exposed the plants to either Mn sufficient or deficient conditions for 9 days. The Mn concentration in roots, young and old leaves was then measured. Under Mn sufficient conditions, Mn concentration in all the tissues did not differ between the six genotypes analyzed (Figure 2a). Under Mn deficient conditions, however, the double mutants accumulated more Mn in roots and less Mn in young leaves than each of the WT and single mutants (Figure 2b). In the old leaves, there was no difference in Mn concentration among all the lines. We also determined Fe and Zn concentrations in these samples and the results showed that in roots and leaves of the double mutants they were similar to those of WT, *nramp1*, *nramp6-1* and *nramp6-2* under both Mn deficient and sufficient conditions (Figure S3). These data suggest that Mn translocation from roots to shoots was only defective in *nramp6nramp1* double mutants. We next assessed Mn concentrations in the two complementation lines and observed full rescue under Mn deficient conditions (Figure S1e), indicating that the loss of *NRAMP6* in the *nramp1* background is responsible for the defect of Mn translocation in the double mutant.

Expression pattern of *NRAMP6* and *NRAMP1*

NRAMP6 was expressed higher in shoots than in roots (Figure 3a and 3b) (Cailliatte *et al.*, 2009, Li *et al.*, 2019). In leaves, *NRAMP6* was more expressed in young tissues than in old tissues (Figure 3a). The expression of *NRAMP6* was not responsive to Mn deficiency in both WT and *nramp1* mutant backgrounds (Figure 3b), nor was it affected by Fe or Zn deficiency (Figure 3c). Compared to *NRAMP1*, *NRAMP6* was expressed at a lower level, particularly in roots (Figure S4a).

To determine the tissue-specific expression pattern of NRAMP6, we made a translational fusion between *NRAMP6* and the β-glucuronidase (GUS)-encoding gene *uidA* under the control of 1.8 kb *NRAMP6* promoter and analyzed GUS expression in Arabidopsis transgenic lines. NRAMP6-GUS was expressed at a low level in roots

and the GUS activity was only detected in root caps and junction sites between lateral roots and primary roots (Figure 3d and 3e). In leaves, NRAMP6-GUS expression was found in whole cotyledons at an early stage (Figure 3f) and was then confined to the major vascular tissues of both cotyledons and true leaves at later stages (Figure 3g) (Cailliatte et al., 2009).

NRAMP1 was previously reported to be mainly expressed in roots (Cailliatte et al., 2010). To determine NRAMP1 expression pattern in shoots, we generated *pNRAMP1:NRAMP1-GUS* transgenic lines. GUS activity was observed in most root tissues with a stronger signal detected in the root tip region (Figure S4b), which is consistent with previous results (Cailliatte et al., 2010). In shoots, GUS activity was strong in whole cotyledons (Figure S4c) and faded in true leaves (Figure S4d).

Loss of *NRAMP6* is required in both roots and shoots for the defective phenotype of *nramp6nramp1*

Although *NRAMP6* was mainly expressed in shoots (Figure 3a and 3b), the double mutants showed defective growth and Mn accumulation in roots. To determine whether *nramp6-1* mutation in shoots contribute to the observed phenotypes in *nramp6-1nramp1*, we performed reciprocal grafting between *nramp1* and *nramp6-1nramp1* mutants. Successfully grafted plants were first cultivated in a nutrient solution with sufficient Mn (10 μM Mn) for 12 days and then subjected to Mn deficiency treatment for 8 days. Mn concentration was then measured in roots, young and old leaves of these grafted plants. Self-grafted *nramp6-1nramp1* showed reduced root growth and Mn translocation from roots to young leaves compared to self-grafted *nramp1* under Mn deficient conditions (Figure 4a and 4b), which is in accordance with the results of nongrafted plants (Figure 1 and 2). Plants with a *nramp6-1nramp1* root stock and a *nramp1* shoot scion or with a *nramp1* root stock and a *nramp1nramp6* shoot scion displayed a similar root growth and Mn translocation capacity to the self-grafted *nramp1* under Mn deficiency (Figure 4a and 4b). These data indicate that mutation of *NRAMP6* in both roots and shoots is required for the defective root growth and Mn translocation in *nramp6-1nramp1*.

We also performed reciprocal grafting between *nramp6-1* and *nramp6-1nramp1* to determine the contribution of the *nramp1* mutation in roots and shoots to the defective phenotypes of *nramp6-1nramp1*. Results showed that plants with a *nramp6-1nramp1* root stock and a *nramp6-1* shoot scion were defective in root growth and Mn translocation from the roots to the young leaves, which is similar to self-grafted *nramp6-1nramp1* (Figure 4c and 4d). This indicates that unlike for *NRAMP6*, the absence of *NRAMP1* expression in the shoot does not contribute to the abnormal phenotype of the double mutant, regardless of Mn supply. Plants with a *nramp6-1* root stock and a *nramp6-1nramp1* shoot scion did not display the double mutant phenotype, which expectedly requires the absence of *NRAMP1* expression in the root. Intriguingly, these plants accumulated more Mn in young leaves than self-grafted *nramp6-1* (Figure 4d).

NRAMP1 can substitute for NRAMP6 to rescue the *nramp6* mutation-induced defective root growth

Since NRAMP6 plays a cooperative role with NRAMP1 to promote root growth and Mn translocation under Mn deficiency, we asked whether the two proteins were exchangeable in the mediation of Mn transport. To that aim, we transformed the *nramp6-1nramp1* double mutant with either one of the constructs *pNRAMP6:NRAMP1-GFP* and *pNRAMP1:NRAMP6-GFP*. Root growth was similar across all the lines under Mn sufficient conditions (Figure 5). Under Mn deficient conditions, *nramp6-1nramp1* slow growth was rescued up to the *nramp1* level by the introduction of the *pNRAMP6:NRAMP1-GFP* transgene (Figure 5a and 5b). In contrast, introduction of *pNRAMP1:NRAMP6-GFP* into the double mutant was unable to recover the deficient root growth of the double mutant to the *nramp6-1* level (Figure 5c and 5d), although the *pNRAMP1:NRAMP6-GFP* transgene could improve the root growth of the double mutant to the *nramp1* level. Quantitative RT-PCR analysis showed that the expression levels of *NRAMP6* in *pNRAMP1:NRAMP6-GFP/nramp6-1nramp1* transgenic lines were comparable to the *NRAMP1* expression level in WT (Figure S5a). The defective recovery of root growth

in the *pNRAMP1:NRAMP6-GFP* lines was not due to the functional deficiency of NRAMP6 fusion with GFP, because *35S:NRAMP6-GFP* could rescue the defective root growth of *nramp6-1nramp1* to the *nramp1* level under Mn deficiency (Figure S5b-d). These results demonstrate that NRAMP1 can substitute for NRAMP6 to regulate root growth, whereas the function of NRAMP1 is not replaceable by the NRAMP6.

Effect of Mn deficiency on protein accumulation and subcellular localization of NRAMP6

The NRAMP6 protein was recently showed to be addressed to Golgi and TGN in protoplasts (Li et al., 2019). To examine NRAMP6 subcellular localization in Arabidopsis, we first examined GFP fluorescence in Arabidopsis protoplasts transiently expressing the *35S:NRAMP6-GFP* construct. We found that NRAMP6-GFP was mainly localized to the ER, which was evidenced by its co-localization with the ER marker RFP-HDEL (Figure S6a). We also fused GFP to the N-terminus of NRAMP6 and investigated the subcellular localization of GFP-NRAMP6. Similarly, GFP-NRAMP6 fluorescence was also predominantly localized to the ER (Figure S6b). To determine the subcellular localization of NRAMP6 in *Arabidopsis* plants, we used the *pNRAMP1:NRAMP6-GFP* and *35S:NRAMP6-GFP* lines with *nramp6-1nramp1* background to observe GFP fluorescence. The expression level of *NRAMP6* in roots of these lines was 15- to 25-fold higher than that in WT (Figure S5a and S5b). However, we could not detect the GFP fluorescence in these transgenic lines.

In order to obtain transgenic lines with high expression level of *NRAMP6*, we changed to use UBQ10 promoter and generated *pUBQ10:NRAMP6-YFP* transgenic lines in *nramp6-1nramp1* background. The expression level of *NRAMP6* in roots of the transgenic lines was around 100-fold higher than in those of WT (Figure S7a). In these lines, we were able to detect YFP fluorescence and found that NRAMP6-YFP fluorescence could be detected in the plasma membrane as well as intracellular membranes, co-localizing in part with the plasma membrane marker FM4-64. The

intracellular membrane-localized NRAMP6-YFP was largely but not completely co-localized with an ER marker SP-mCherry-HDEL (Figure S6c). Interestingly, Mn deficiency was able to induce the accumulation of NRAMP6-YFP and promote the localization of NRAMP6-YFP to the plasma membrane (Figure 6a and 6b).

We also generated *pUBQ10:NRAMP6-HA* transgenic lines in *nramp6-1nramp1* background. The *NRAMP6* expression level in roots of the *pUBQ10:NRAMP6-HA* transgenic lines was nearly 1,000 times higher than in those of WT (Figure S7b). Immunoblot analysis using anti-HA antibody showed that Mn deficiency increased NRAMP6-HA protein level in the roots, but reduced its accumulation in the shoots (Figure 6c). To confirm this observation, we performed immunoblot analysis of NRAMP6-HA in two *pNRAMP6:NRAMP6-HA* transgenic lines with *nramp1* background. Although NRAMP6-HA protein was not detected in the roots of the two lines under Mn sufficient conditions, it could be detected in the roots under Mn deficient conditions (Figure 6d). In contrast, Mn deficiency reduced the protein accumulation of NRAMP6-HA in the shoots (Figure 6d). These results revealed that Mn plays an opposite role in the regulation of NRAMP6 protein accumulation between roots and shoots.

We then analyzed the subcellular localization of NRAMP6-HA of the *pUBQ10:NRAMP6-HA* transgenic lines by aqueous two-phase partitioning. Aqueous two-phase partitioning in polyethylene glycol-Dextran mixtures can make around 90% of the plasma membrane and 80-90% of the intracellular membranes partitioned to the upper phase and the lower phase, respectively (Larsson *et al.*, 1987, DeWitt *et al.*, 1996). Consistently, our aqueous two-phase partitioning experiments showed that the plasma membrane (H^+-ATPase) and ER (BiP) markers enriched to the upper phase and the lower phase, respectively (Figure 6e). NRAMP6-HA was found to be present at both the upper and lower phases in roots and shoots under Mn sufficient conditions, albeit preferentially existed at the lower phase especially in the roots (Figure 6e). Interestingly, Mn deficiency remarkably promoted the accumulation of NRAMP6-HA to the upper phase in the roots (Figure 6e). Together, these results demonstrate that Mn deficiency increases NRAMP6 protein level in the roots while reduces its

accumulation in the shoots, and promotes the localization of NRAMP6 to the plasma membrane.

NRAMP6 can rescue the defective growth of yeast Δ*smf2* under Mn deficiency

To examine whether NRAMP6 has Mn transport capacity, we expressed *NRAMP6* in the yeast strains Δ*smf1* and Δ*smf2* that are defective in Mn uptake and endomembrane Mn transport, respectively (Supek *et al.*, 1996, Cohen *et al.*, 2000). Under Mn sufficient conditions, *NRAMP6*-expressing yeast cells could grow at a similar speed to control cells harboring the empty vector (Figure 7). Under Mn deficiency, while the expression of *NRAMP6* did not rescue growth of Δ*smf1* yeast cells, *NRAMP6* expression in Δ*smf2* cells was able to restore it substantially (Figure 7). Previously, NRAMP6 was demonstrated to be localized to the endomembrane compartment instead of the plasma membrane of the yeast cells (Cailliatte et al., 2009). These results thus suggest that NRAMP6 can function as an endomembrane Mn transporter in yeast.

Discussion

NRAMP family members in plants are reported to have a broad range of metal substrates, including Mn, Fe and Cd (Lanquar *et al.*, 2005, Cailliatte *et al.*, 2010, Lanquar *et al.*, 2010, Sasaki *et al.*, 2012, Castaings *et al.*, 2016). NRAMP6 was previously reported to function as a Cd transporter to contribute to Cd toxicity in *Arabidopsis* (Cailliatte et al., 2009), and recently it was also characterized as a Fe transporter to regulate plant growth under Fe-deficient conditions (Li et al., 2019). However, whether NRAMP6 plays a role in Mn nutrition in *Arabidopsis* was still unclear. In this study, we demonstrate that NRAMP6 can function as a Mn transporter to modulate root growth and Mn translocation under Mn deficiency. Although *nramp6* single mutants do not show any defective phenotypes under Mn deficient conditions, simultaneous inactivation of *NRAMP6* and *NRAMP1* genes enhances the root growth inhibition phenotype of the *nramp1* single mutant in response to Mn deficiency

(Figure 1). Since the expression level of *NRAMP1* is remarkably higher than that of *NRAMP6* (Figure S4a), these results suggest that NRAMP6 and NRAMP1 have overlapping functions in the plant tolerance to Mn deficiency, with NRAMP1 being the major player.

A previous study established that NRAMP1 is required for Mn acquisition by the roots (Cailliatte et al., 2010). In this study we demonstrate that NRAMP1 also plays a cooperative role with NRAMP6 in the translocation of Mn from roots to shoots (Figure 2). The exact mechanism as to how NRAMP1 and NRAMP6 cooperatively mediate Mn translocation is still unknown. Grafting experiments reveal that mutation of *NRAMP6* in both roots and shoots is required for the defective root growth and Mn translocation in *nramp1nramp6* (Figure 4), while mutation of *NRAMP1* only in the roots is required for defective phenotypes in the double mutant. These results suggest that the *nramp6* mutation in the shoots might elicit and transmit a signal from the shoots to the roots to regulate root growth and Mn transport. Interestingly, plants harboring a root stock of *nramp6-1* and a shoot scion of *nramp6-1nramp1* accumulated a higher level of Mn in young leaves than self-grafted *nramp6-1* (Figrue 4d), which suggests that the shoots of *nramp6-1nramp1* might experience Mn deficiency and transmit a signal to the roots and promotes Mn transport to the shoots, although the exact underlying mechanism remains elusive. Our data also imply the existence of long distance shoot-to-root signaling in plants subjected to Mn deficiency.

Although *NRAMP6* is mainly expressed in the shoots (Figure 3), the lower expression of *NRAMP6* in the roots is required for root growth and Mn translocation under Mn deficient conditions. The mRNA expression of *NRAMP6* was not responsive to Mn deficiency in both WT and *nramp1* background (Figure 3b and 3c). Nevertheless, we found that the protein level of NRAMP6-HA under the control of both *UBQ10* and *NRAMP6* native promoters was increased in the roots while decreased in the shoots under Mn deficiency (Figure 6c and 6d). Moreover, Mn deficiency promotes the NRAMP6-YFP and NRAMP6-HA accumulation to the plasma membrane (Figure 6e). Together, these results reveal that plants can increase

the total level of NRAMP6 protein and its localization to the plasma membrane to compensate the defective Mn uptake and/or translocation of *nramp1* when environmental Mn availability is low. On the other hand, the expression of *NRAMP6* in vascular tissues of the shoots implies that NRAMP6 in the shoots might play a role in unloading Mn from the roots and/or the remobilization of Mn from old leaves to young tissues. Under Mn deficient conditions, the reduction of NRAMP6 protein level in the shoots may help the retention of more Mn in the roots to preferentially sustain root growth.

NRAMP6-GFP was previously shown to be localized to the Golgi in *Arabidopsis* protoplasts (Li et al., 2019), but we found that both NRAMP6-GFP and GFP-NRAMP6 are mainly localized to the ER in the *Arabidopsis* protoplasts (Figure S6). The reason for the different results of NRAMP6-GFP subcellular localization between the previous report and this study is currently unknown. In *Arabidopsis* plants, NRAMP6 was found to be localized in both the plasma membrane and ER, and its localization to the plasma membrane was enhanced under Mn deficiency (Figure 6a and 6b). In accordance with the partial localization of NRAMP6 to the plasma membrane, the plasma membrane-localized NRAMP1 can substitute for NRAMP6 to rescue the defective root growth of *nramp6-1nramp1* (Figure 5a and 5b) and NRAMP6 plays a cooperative role with NRAMP1 but not with the Golgi-localized NRAMP2 in the regulation of root growth under Mn deficiency (Figure 1; Figure S2). The replaceable function of NRAMP6 by NRAMP1 also suggests that the plasma membrane-localized portion of NRAMP6 is involved in the regulation of root growth and Mn accumulation under Mn deficient conditions. The dual localization of NRAMP6 might also explain the lack of full recovery of *nramp6nramp1* root growth by the *pNRAMP1:NRAMP6-GFP* transgene under Mn deficiency (Figure 5c and 5d), although we can not exclude the possibility that NRAMP6 has a different Mn transport activity or protein stability from NRAMP1. In the future, it would be interesting to determine how Mn deficiency regulates *NRAMP6* at a post-transcriptional level.

EXPERIMENTAL PROCEDURES

Plant materials and growth conditions

Arabidopsis thaliana (Columbia ecotype, Col-0) was used as the wild-type for all the control experiments. The T-DNA insertion lines *nramp6-1* (GK-550D06) and *nramp1* (SALK_053236C) were derived from uNASC (http://szlapncs01.nottingham.ac.uk/). *nramp2* mutant was obtained from our previous work (Gao et al., 2018). To generate an additional mutant allele of *NRAMP6*, the CRISPR/Cas9-based genome editing method was used. Two 20-bp coding sequences (Table S1) of *NRAMP6* were constructed into a sgRNA-Cas9 expression vector (Ma and Liu, 2016) and transformed into Col-0 WT background. After sequencing the target region of *NRAMP6* in T3 transgenic lines without Cas9-transgene, a mutant allele (*nramp6-2*) was identified, which has 1-bp insertion at 15 bp from the start codon of *NRAMP6*.

Seeds were sterilized by 8% sodium hypochlorite and then stratified for 3 d at 4°C for plant growth in agar plates. The agar medium consists of 2% sucrose, 1% agar (A1296, Sigma-Aldrich), and full-strength Hoagland nutrient solution (5 mM KNO_3, 5 mM $CaNO_3$, 2 mM $MgSO_4$, 1 mM $NH_4H_2PO_4$, 3 μM H_3BO_3, 1 μM $(NH_4)_6Mo_7O_{24}$, 0.4 μM $ZnSO_4$, 0.2 μM $CuSO_4$, 20 μM Fe(III)-EDTA) containing various concentrations of $MnSO_4$ at pH 5.7. For hydroponic cultures, seeds were directly grown a plastic mesh floating on one-tenth strength Hoagland nutrient solution and the solution was renewed every two to three days. Plants were grown in a growth chamber with 14 h of light and 10 h of darkness at 22°C.

Evaluation of root growth in response to Mn deficiency

Seedlings were grown on a nutrient agar plate containing 0, 0.5, 2, 5, or 10 μM $MnSO_4$. After growth for 7 d, the seedlings were photographed and compared. The root length was measured using ImageJ software. Root hairs in the mature zones of the roots were photographed by a stereo microscope (SZX12, Olympus) equipped with a camera (DP20, Olympus) and measured for their lengths by ImageJ.

Measurement of cation concentration

Seeds were grown on a 1/10 strength Hoagland nutrient solution containing 10 μM $MnSO_4$ for 18 d and then the plants were exposed to the same Hoagland nutrient solution containing 0 or 10 μM $MnSO_4$ for 9 d. Roots, young leaves (three to four top unexpanded leaves) and old leaves (fully expanded leaves) were sampled after the roots were washed with a solution of 2 mM $CaSO_4$ and 10 mM EDTA for 10 min to remove apoplastic Mn and subsequently rinsed with ultra-pure water for three times. The samples were dried at 65°C for more than 3 d and digested with concentrated HNO_3 and then diluted with 2% HNO_3. The concentrations of Mn, Zn or Fe in the diluted solution were determined using inductively coupled plasma mass spectrometry (ICP-MS; PerkinElmer NexION300D).

Grafting experiments

Sterilized and stratified seeds of *nramp1*, *nramp6-1* and *nramp6-1nramp1* were grown on an agar medium consisting of 1.2% agar, 1/2 MS medium plus 0.1% vitamins (M519, PhytoTech Labs), 0.04 ppm 6-benzylaminopurine (B3408, Sigma-Aldrich), 0.02 ppm IAA (I2886, Sigma-Aldrich), 3 ppm BEN (381586, Sigma-Aldrich), and 2% sucrose. After growth for 4 d, the seedlings were kept in the dark for 2 d to promote hypocotyl elongation. Subsequently, the seedlings with approximately equal hypocotyl diameters and developmental stages were excised with a 15° stab knife (SAR POINT REF 72-1501) and then shoot scions and root stocks were grafted. The grafted seedlings were grown on the agar medium for 6 d for recovery. The successfully grafted plants were then transferred to a 1/10 strength Hoagland nutrient solution containing 10 μM $MnSO_4$ for a hydroponic culture. After growth for 12 d, the plants were treated with the Hoagland nutrient solution containing 0 or 10 μM $MnSO_4$ for 8 d. The Mn concentrations in roots, young and old leaves were determined by ICP-MS.

Complementation analysis

To perform complementation test of *nramp6-1nramp1* mutant, a DNA fragment harboring 1.8 kb promoter, the gene and 1.0 kb downstream of stop codon of

NRAMP6 (AT1G15960) was amplified and cloned into a binary vector pCAMBIA3301. The resultant vector was transformed into *nramp6-1nramp1* by *Agrobacterium*-mediated floral dip method. T3 homozygous plants harboring the transgene were subjected for root growth assay, root hair observation and Mn accumulation analysis.

To examine whether NRAMP6 fused with GFP is functional in vivo, *NRAMP6* was amplified and inserted into pCAMBIA1301 vector that harbors *35S* promoter and *GFP* sequence. The resultant vector containing *35S:NRAMP6-GFP* was transformed into *nramp6-1nramp1* mutant. T3 homozygous plants harboring the transgene were subjected for root growth assay.

To investigate whether NRAMP1 and NRAMP6 proteins can substitute each other to be functional in plants, we constructed *pNRAMP1:NRAMP6-GFP* and *pNRAMP6:NRAMP1-GFP* vectors. For the construct of *pNRAMP1:NRAMP6-GFP*, the 1.65 kb *NRAMP1* promoter and *NRAMP6* coding sequence without a stop codon were amplified, respectively, and then fused to one fragment by overlapping PCR and cloned into the pCAMBIA1301 vector harboring *GFP* sequence. For the construct of *pNRAMP6:NRAMP1-GFP*, the 1.8 kb *NRAMP6* promoter and *NRAMP1* coding sequence without a stop codon were amplified and fused, and then inserted into the same pCAMBIA1301 vector harboring the *GFP* sequence. The two constructs were transformed into *nramp6-1nramp1* mutant, respectively, and T3 homozygous plants harboring each transgene were subjected for root growth assay. The primers for all the vector constructs can be found in Table S1.

mRNA expression analysis

To examine the expression pattern of *NRAMP6*, different tissues including roots, young and old leaves were excised for RNA extraction. For the expression analysis of *NRAMP6* in response to Mn, seeds of WT and *nramp1* mutant were sown on a nutrient agar medium with or without 10 μM $MnSO_4$ for 7 d growth and the roots and shoots were harvested for RNA isolation. For the expression analysis of *NRAMP6* under Fe or Zn deficient conditions, 20-day-old plants of WT were exposed to 1/10

strength Hoagland nutrient solution without Zn or Fe for 7 d. Total RNA of each sample was extracted using the TaKaRa M iniBEST plant RNA Extraction Kit (Cat # 9769). Approximately 1 μg of total RNA was first digested with DNase I and then used for the synthesis of first-strand cDNAs by using the HiScript® 1st Strand cDNA Synthesis Kit (Vazyme Biotech Co., Ltd., Nanjing, China). One-twentieth of the cDNA products were used for RT-PCR and real-time RT-PCR analysis. For the real-time RT-PCR analysis, the SYBR® Green Master Mix kit (Vazyme Biotech Co., Ltd., Nanjing, China) was used. *UBQ10* was used as an internal control. The expression levels of *NRAMP6* and *NRAMP1* was first normalized to *UBQ10* control and then normalized to *NRAMP6* level in roots under Mn sufficient conditions. The detailed information of the primers used for expression analysis are listed Table S1. Real-time RT-PCR data were collected in accordance with the CFX96 Touch real-time PCR detection system (BioRad).

GUS analysis

To generate *pNRAMP6:NRAMP6-GUS* and *pNRAMP1:NRAMP1-GUS* transgenic lines, 1.8-kb promoter plus the gene of *NRAMP6* and 2.0-kb promoter plus the gene of *NRAMP1* without their stop codons were amplified and fused in frame to *GUS* reporter gene in pORE-R2 vector, respectively. T3 transgenic plants containing the homozygous *pNRAMP6:NRAMP6-GUS* or *pNRAMP1:NRAMP1-GUS* were selected for GUS analysis. For *pNRAMP6:NRAMP6-GUS* transgenic lines, roots and shoots were then stained with a commercialized GUS staining solution (161031; o'Biolab Co., Ltd., Beijing, China) for overnight at 37□. For *pNRAMP1:NRAMP1-GUS* transgenic lines, roots were stained for 45 min to 1 h, while shoots were stained for overnight at 37□. Stained shoot samples were subjected to an ethanol series (20%, 35%, 50% and 70%) to remove chlorophylls. Stained tissues were observed with a stereomicroscope (SZX7, Olympus) and photographed with a DP26 camera (Olympus).

Subcellular localization analysis

To determine the subcellular localization of NRAMP6 in protoplasts, the *NRAMP6* coding sequence was amplified and fused in frame to *GFP* at the N- or C-terminals of *NRAMP6* and then the fused sequences were, respectively, inserted into a pBluescript vector harboring the *35S* promoter. The resultant vectors containing *35S:NRAMP6-GFP* or *35S:GFP-NRAMP6* were co-transformed with the ER marker *35S: RFP-HDEL* into *Arabidopsis* protoplasts for fluorescence observation using a confocal Zeiss microscope (Zeiss LSM 880). *Arabidopsis* protoplasts were isolated from 14-day-old seedlings according to a previous method (Zhai et al., 2009) and 10 μg of each plasmid DNA was used for protoplast transformation by the polyethylene glycol method.

To investigate the subcellular localization of NRAMP6 in plants, we made the *pUBQ10:NRAMP6-YFP* fusion fragment by PCR using overlapping primers and then inserted the fragment into pCAMBIA1305 vector. The resultant vector was transformed into *nramp6-1nramp1* background. T3 transgenic lines harboring the homogzygous transgene were grown on the nutrient agar plate containing 0 or 10μM $MnSO_4$ for 7 d and then subjected to expression analysis and YFP fluorescence observation by the confocal microscope. We also fused *pUBQ10:NRAMP6* or *pNRAMP6:NRAMP6* fragments with *3×HA* and cloned them into the pCAMBIA1305 vector, and the resultant vectors were then transformed into *nramp6-1nramp1* or *nramp1* mutant backgrounds. T3 seedlings were grown on a 1/10 strength Hoagland nutrient solution containing 10 μM $MnSO_4$ for 18 d and subsequently exposed to the same nutrient solution with or without 10 μM $MnSO_4$ for 9 d. Roots and shoots of the T3 plants were then excised for total protein extraction or microsomal membrane isolation. Microsomal membranes were extracted by using homogenization buffer consisting of 0.29 M sucrose, 25 mM HEPES (pH =8.5), 20 mM EDTA, Polyvinylpyrrolidone K40 (P0507-50g; Sangon), 0.2% BSA, 3 mM DTT, 50 μM MG132, 100 μM PMSF (not AP assay), and 1×complete protease inhibitor mixture EDTA-free (5892791001; Roche). The homogenate was centrifuged at 8,000 g for 15 min at 4 □ and the derived supernatant was then centrifuged at 100,000 g to obtain the microsomal pellet. Aqueous two-phase partitioning was performed using a 20%

dextran and 40% PEG3350 mixture and centrifuging at 1,500 g for 5 min. Immunoblot blot analysis was carried out to determine NRAMP6-HA protein level using anti HA-HRP antibody (12013819001; Roche). The Actin, H^+-ATPase and BiP proteins were used as controls, which were detected by anti-Actin (CW0264M; CoWin Biosciences Co., Ltd., China), anti- H^+-ATPase (Hayashi et al., 2010) and anti-BiP (PHY2155S; PhytoAB) antibodies, respectively. The sequence information of the primers used for the vector constructs are listed Table S1.

Yeast experiments

The coding sequence of *NRAMP6* was amplified and cloned into yeast vector pYC2, which is a low-copy number plasmid and has a galactose-inducible promoter GAL1. The NRAMP6-pYC2 and pYC2 empty vectors were, respectively, transformed into wild-type yeast strain BY4741 (*MATa; his3, leu2, met15, ura3*), and two mutant strains *Δsmf1* (*MATa; his3, leu2, met15, ura3, smf1::kanMX4*) and *Δsmf2* (*MATa; his3, leu2, met15, ura3, smf2::kanMX4*). Yeast cells of each strain were grown in 2% glucose-containing SD liquid mediums without uracil at 30□ for overnight and then the yeast cells were harvested and washed with water for three times. The derived yeast cells were resuspended with water and adjusted to OD_{600}=0.6. Aliquots of 10-fold serial dilutions were dropped on 2% agar SD-Ura medium supplemented with or without 5 mM EGTA.

Statistical analysis

One-way ANOVA followed by Tukey test was used for the statistical analysis of all the quantitative data except for the data of Figure 6b in which two-tailed student's *t* test was used for the statistical analysis.

DATA AVAILABILITY STATEMENT

Sequence data in this article can be found in the *Arabidopsis* Information Resource (TAIR) database under the following accession number: At1g15960 for *NRAMP6*,

At1g80830 for *NRAMP1* and At1g80830 for *NRAMP2*.

ACKNOWLEDGEMENTS

We thank Prof. Toshinori Kinoshita from Nagoya University for kindly providing the anti-H^+-ATPase antibody. This work was supported by the National Natural Science Foundation of China (Grant No. 31900217), the Shanghai Center for Plant Stress Biology, Chinese Academy of Sciences, and National Key Laboratory of Plant Molecular Genetics, and by Grant-in-Aid for Specially Promoted Research (JSPS KAKENHI Grant Number 16H06296 to J.F.M.).

AUTHOR CONTRIBUTIONS

LL, ZZ, YL, and C-FH designed the experiments; LL, ZZ, YL, CY, NF, JZ, NY, LD, and JFM performed the experiments; JFM, and CC commented on this work; LL, ZZ and C-FH analyzed the data and prepared figures; C-FH wrote the manuscript.

CONFLICT OF INTEREST

The authors declare no competing interests.

SUPPORTING INFORMATION

Figure S1. Complementation test of *nramp6-1nramp1*.

Figure S2. NRAMP6 does not play a redundant role with NRAMP2 in the regulation of root growth under Mn deficiency.

Figure S3. Mutation of *NRAMP6* does not affect Fe and Zn accumulation.

Figure S4. Expression analysis of *NRAMP1* and *NRAMP6*.

Figure S5. Overexpression of *NRAMP6-GFP* can complement the defective root growth of *nramp6-1nramp1* under Mn deficiency.

Figure S6. Subcellular localization of NRAMP6 in Arabidopsis.

Figure S7. Expression analysis of *NRAMP6* in UBQ10 promoter-driven *NRAMP6* overexpression lines.

Table S1. The list of primers used in this study.

REFERENCES

Alejandro, S., Cailliatte, R., Alcon, C., Dirick, L., Domergue, F., Correia, D., Castaings, L., Briat, J.F., Mari, S. and Curie, C. (2017) Intracellular distribution of manganese by the trans-Golgi network Transporter NRAMP2 is critical for photosynthesis and cellular redox homeostasis. *Plant Cell*, **29**, 3068-3084.

Cailliatte, R., Lapeyre, B., Briat, J.F., Mari, S. and Curie, C. (2009) The NRAMP6 metal transporter contributes to cadmium toxicity. *Biochem. J.*, **422**, 217-228.

Cailliatte, R., Schikora, A., Briat, J.F., Mari, S. and Curie, C. (2010) High-affinity manganese uptake by the metal transporter NRAMP1 is essential for *Arabidopsis* growth in low manganese conditions. *Plant Cell*, **22**, 904-917.

Castaings, L., Caquot, A., Loubet, S. and Curie, C. (2016) The high-affinity metal transporters NRAMP1 and IRT1 team up to take up iron under sufficient metal provision. *Sci. Rep.*, **6**, 37222.

Cohen, A., Nelson, H. and Nelson, N. (2000) The family of SMF metal ion transporters in yeast cells. *J. Biol. Chem.*, **275**, 33388-33394.

DeWitt, N.D., Hong, B.M., Sussman, M.R. and Harper, J.F. (1996) Targeting of two Arabidopsis H^+-ATPase isoforms to the plasma membrane. *Plant Physiol.*, **112**, 833-844.

Eisenhut, M., Hoecker, N., Schmidt, S.B., Basgaran, R.M., Flachbart, S., Jahns, P., Eser, T., Geimer, S., Husted, S., Webers, A.P.M., Leister, D. and Schneider, A. (2018) The plastid envelope CHLOROPLAST MANGANESE TRANSPORTER1 is essential for manganese homeostasis in *Arabidopsis*. *Mol. Plant*, **11**, 955-969.

Forde, B.G. (2002) Local and long-range signaling pathways regulating plant responses to nitrate. *Annu. Rev. Plant Biol.*, **53**, 203-224.

Gao, H.L., Xie, W.X., Yang, C.H., Xu, J.Y., Li, J.J., Wang, H., Chen, X. and Huang, C.F. (2018) NRAMP2, a trans-Golgi network-localized manganese transporter, is required for *Arabidopsis* root growth under manganese deficiency. *New Phytol.*, **217**, 179-193.

Grillet, L., Lan, P., Li, W.F., Mokkapati, G. and Schmidt, W. (2018) IRON MAN is a ubiquitous family of peptides that control iron transport in plants. *Nat Plants*, **4**, 953-+.

Grusak, M.A. and Pezeshgi, S. (1996) Shoot-to-root signal transmission regulates root Fe(III) reductase activity in the dgl mutant of pea. *Plant Physiol.*, **110**, 329-334.

Hayashi, Y., Nakamura, S., Takemiya, A., Takahashi, Y., Shimazaki, K. and Kinoshita, T. (2010) Biochemical characterization of in vitro phosphorylation and dephosphorylation of the plasma membrane H^+-ATPase. *Plant Cell Physiol.*, **51**, 1186-1196.

Hirayama, T., Lei, G.J., Yamaji, N., Nakagawa, N. and Ma, J.F. (2018) The putative peptide gene *FEP1* regulates iron deficiency response in Arabidopsis. *Plant Cell Physiol.*, **59**, 1739-1752.

Ko, D. and Helariutta, Y. (2017) Shoot-root communication in flowering plants. *Curr. Biol.*, **27**, R973-R978.

Korshunova, Y.O., Eide, D., Clark, W.G., Guerinot, M.L. and Pakrasi, H.B. (1999) The IRT1 protein from *Arabidopsis thaliana* is a metal transporter with a broad substrate range. *Plant Mol. Biol.*, **40**, 37-44.

Lanquar, V., Lelievre, F., Bolte, S., Hames, C., Alcon, C., Neumann, D., Vansuyt, G., Curie, C., Schroder, A., Kramer, U., Barbier-Brygoo, H. and Thomine, S. (2005) Mobilization of vacuolar iron by AtNRAMP3 and AtNRAMP4 is essential for seed germination on low iron. *EMBO J.*, **24**, 4041-4051.

Lanquar, V., Ramos, M.S., Lelievre, F., Barbier-Brygoo, H., Krieger-Liszkay, A., Kramer, U. and Thomine, S. (2010) Export of vacuolar manganese by AtNRAMP3 and AtNRAMP4 is required for optimal photosynthesis and growth under manganese deficiency. *Plant Physiol.*, **152**, 1986-1999.

Larsson, C., Widell, S. and Kjellbom, P. (1987) Preparation of high-purity plasma membranes. *Methods Enzymol.*, **148**, 558-568.

Li, J.Y., Wang, Y.R., Zheng, L., Li, Y., Zhou, X.L., Li, J.J., Gu, D.F., Xu, E.D., Lu, Y.P., Chen, X. and Zhang, W. (2019) The intracellular transporter AtNRAMP6 is involved in Fe homeostasis in *Arabidopsis*. *Front. Plant Sci.*, **10**, 1124.

Liu, T.Y., Chang, C.Y. and Chiou, T.J. (2009) The long-distance signaling of mineral macronutrients. *Curr. Opin. Plant Biol.*, **12**, 312-319.

Ma, X. and Liu, Y.G. (2016) CRISPR/Cas9-based multiplex genome editing in monocot and dicot plants. *Curr. Protoc. Mol. Biol.*, **115**, 31.36.31-31.36.21.

Marschner, H. (2012) *Mineral nutrition of Higher plants* 3 edn. London: Academic Press.

Mills, R.F., Doherty, M.L., Lopez-Marques, R.L., Weimar, T., Dupree, P., Palmgren, M.G., Pittman, J.K. and Williams, L.E. (2008) ECA3, a Golgi-localized P_{2A}-type ATPase, plays a crucial role in manganese nutrition in Arabidopsis. *Plant Physiol.*, **146**, 116-128.

Milner, M.J., Seamon, J., Craft, E. and Kochian, L.V. (2013) Transport properties of members of the ZIP family in plants and their role in Zn and Mn homeostasis. *J. Exp. Bot.*, **64**, 369-381.

Rogers, E.E. and Guerinot, M.L. (2002) FRD3, a member of the multidrug and toxin efflux family, controls iron deficiency responses in Arabidopsis. *Plant Cell*, **14**, 1787-1799.

Sasaki, A., Yamaji, N., Yokosho, K. and Ma, J.F. (2012) Nramp5 is a major transporter responsible for manganese and cadmium uptake in rice. *Plant Cell*, **24**, 2155-2167.

Schmidt, S.B., Jensen, P.E. and Husted, S. (2016) Manganese deficiency in plants: the impact on photosystem II. *Trends Plant Sci.*, **21**, 622-632.

Schneider, A., Steinberger, I., Herdean, A., Gandini, C., Eisenhut, M., Kurz, S., Morper, A., Hoecker, N., Ruhle, T., Labs, M., Flugge, U.I., Geimer, S., Schmidt, S.B., Husted, S., Weber, A.P.M., Spetea, C. and Leister, D. (2016) The evolutionarily conserved protein PHOTOSYNTHESIS AFFECTED MUTANT71 is required for efficient manganese uptake at the thylakoid membrane in Arabidopsis. *Plant Cell*, **28**, 892-910.

Supek, F., Supekova, L., Nelson, H. and Nelson, N. (1996) A yeast manganese transporter related to the macrophage protein involved in conferring resistance to mycobacteria. *Proc. Natl. Acad. Sci. U.S.A.*, **93**, 5105-5110.

Tabata, R., Sumida, K., Yoshii, T., Ohyama, K., Shinohara, H. and Matsubayashi, Y. (2014) Perception of root-derived peptides by shoot LRR-RKs mediates systemic N-demand signaling. *Science*, **346**, 343-346.

Ueno, D., Sasaki, A., Yamaji, N., Miyaji, T., Fujii, Y., Takemoto, Y., Moriyama, S., Che, J., Moriyama, Y., Iwasaki, K. and Ma, J.F. (2015) A polarly localized transporter for efficient manganese uptake in rice. *Nat Plants*, **1**, 15170.

Vert, G., Grotz, N., Dedaldechamp, F., Gaymard, F., Guerinot, M.L., Briat, J.F. and Curie, C.

(2002) IRT1, an *Arabidopsis* transporter essential for iron uptake from the soil and for plant growth. *Plant Cell*, **14**, 1223-1233.

Yamaji, N., Sasaki, A., Xia, J.X., Yokosho, K. and Ma, J.F. (2013) A node-based switch for preferential distribution of manganese in rice. *Nat. Commun.*, **4:2442**.

Yang, C.H., Wang, C., Singh, S., Fan, N., Liu, S., Zhao, L., Cao, H.L., Xie, W.X., Yang, C.W. and Huang, C.F. (2021) Golgi-localised manganese transporter PML3 regulates *Arabidopsis* growth through modulating Golgi glycosylation and cell wall biosynthesis. *New Phytol.*, **231**, 2200-2214.

Yang, M., Zhang, Y.Y., Zhang, L.J., Hu, J.T., Zhang, X., Lu, K., Dong, H.X., Wang, D.J., Zhao, F.J., Huang, C.F. and Lian, X.M. (2014) OsNRAMP5 contributes to manganese translocation and distribution in rice shoots. *J. Exp. Bot.*, **65**, 4849-4861.

Zhai, Z., Jung, H.I. and Vatamaniuk, O.K. (2009) Isolation of protoplasts from tissues of 14-day-old seedlings of *Arabidopsis thaliana*. *J Vis Exp*, 1149.

Zhang, B., Zhang, C., Liu, C.G., Jing, Y.P., Wang, Y., Jin, L., Yang, L., Fu, A.G., Shi, J.S., Zhao, F.G., Lan, W.Z. and Luan, S. (2018) Inner envelope CHLOROPLAST MANGANESE TRANSPORTER 1 supports manganese homeostasis and phototrophic growth in *Arabidopsis*. *Mol. Plant*, **11**, 943-954.

FIGURE LEGENDS

Figure 1. Mutation of *NRAMP6* in *nramp1* background reduces root growth and root hair elongation at low Mn conditions.

(a) Gene structure and mutation sites of *NRAMP6*. Black boxes and horizontal lines between the boxes indicate exons and introns, respectively. *nramp6-1* and *nramp6-2* have a T-DNA insertion in intron 7 and 1-bp insertion located 15 bp downstream of the start codon of *NRAMP6*, respectively.

(b)–(e) Phenotypes of root growth (b and c) and root hair elongation (d and e) at low Mn conditions. Seeds of WT, *nramp1*, *nramp6-1*, *nramp6-1nramp1*, *nramp6-2*, and *nramp6-2nramp1* were grown at a nutrient agar plate containing 0, 0.5, 2, 5, or 10 μM. After growth for 7 d, the roots were photographed for root length and root hair measurement. Scale bar=500 μm. Data shown are means ± SD of 10 to 12 root lengths (c) and of around 100 root hair lengths (e). Different letters at each treatment indicate values significantly different ($P<0.05$, ANOVA followed by Tukey test).

Figure 2. Mn translocation from roots to shoots is impaired in *nramp6nramp1* double mutants.

(a), (b) Mn accumulation in roots, young leaves and old leaves under Mn-sufficient (a) or –deficient (b) conditions. Eighteen-day-old plants of WT, *nramp1*, *nramp6-1*, *nramp6-1nramp1*, *nramp6-2*, and *nramp6-2nramp1* were treated with 0 (b) or 10 μM Mn (a) for 9 d. Roots, young leaves (3-4 top unexpanded leaves) and old leaves (fully expanded leaves) were then harvested for the determination of Mn concentrations. Data shown are means ± SD of four biological replicates. Different letters at each treatment indicate values significantly different ($P<0.05$, ANOVA followed by Tukey test).

Figure 3. Expression pattern of *NRAMP6*.

(a) Expression analysis of *NRAMP6* in roots, young leaves and old leaves.

(b) Expression of *NRAMP6* in WT and *nramp1* backgrounds in response to Mn deficiency. Seedlings of WT and *nramp1* were grown on a nutrient agar plate with 0 (-Mn) or 10 μM Mn (+Mn) for 7 d. and then roots and shoots were harvested for RNA isolation and expression analysis.

(c) Expression of *NRAMP6* in WT background in response to Fe or Zn deficiency. Twenty-day-old plants were exposed to a nutrient solution with or without Fe or Zn for 7 d.

(d)–(g) Detection of GUS activity in *pNRAMP6:NRAMP6-GUS* transgenic lines. GUS expression was detected in root caps (d) and the junction sites of lateral roots and primary roots (e). (f and g) GUS activity was found in whole cotyledons at early stages (f) and the major vascular tissues of both cotyledons and true leaves at later stages (g). Scale bar=200 μm. Values are means ±SD of three (a and b) or four (c) biological replicates. Means with different letters are significantly different ($P<0.05$, ANOVA followed by Tukey test).

Figure 4. Root biomass and Mn accumulation in grafted plants under Mn deficiency.

(a), (b) root biomass (a) and Mn concentration (b) in the grafted plants between *nramp1* (*nr1*) and *nramp6-1nramp1* (*nr6nr1*). Successfully grafted seedlings of *nr1*/*nr1*, *nr6nr1*/*nr6nr1*, *nr6nr1*/*nr1*, and *nr1*/*nr6nr1* (shoot/root) were cultured in

nutrient agar plates for 6 d for the recovery and subsequently transferred to grow on a nutrient solution containing 10 μM Mn for 12 d. The plants were then treated with 0 (-Mn) or 10 μM Mn (+Mn) for 9 d. Root biomass and Mn concentrations in roots, young leaves and old leaves were determined and compared in the four grafted lines. (c), (d) root biomass (c) and Mn concentration (d) in the grafted plants between *nramp6* (*nr6*) and *nramp6-1nramp1* (*nr6nr1*). Grafted plants of *nr6*/*nr6*, *nr6nr1*/*nr6nr1*, *nr6*/*nr6nr1*, and *nr6nr1*/*nr6* (shoot/root) were treated with or without 10 μM Mn for 8 d to determine their root biomass and Mn concentrations in the roots, young leaves and old leaves. Values are means ±SD of four biological replicates. Means with different letters are significantly different ($P<0.05$, ANOVA followed by Tukey test). Two independent experiments were performed with similar results.

Figure 5. NRAMP1 can replace NRAMP6 to regulate root growth, but not vice versa. (a), (b) Rescue of the defective root growth of *nramp6-1nramp1* by *pNRAMP6:NRAMP1-GFP* (*pNR6:NR1-GFP*). Seedlings of WT, *nramp1*, *nramp6-1*, *nramp6-1nramp1*, and two *pNR6:NR1-GFP* transgenic lines in *nramp6-1nramp1* background were grown on a nutrient agar plate with 0 (-Mn) or 10 μM Mn (+Mn) for 7 d. The seedlings were photographed and compared (a), and root lengths were measured and quantified (b).

(c), (d) Images (c) and quantitative data (d) of root growth phenotype in WT, *nramp1*, *nramp6-1*, *nramp6-1nramp1*, and two *pNRAMP1:NRAMP6-GFP* (*pNR1:NR6-GFP*) transgenic lines in *nramp6-1nramp1* background. Data shown are means ± SD of 10 primary root lengths. Different letters at each treatment indicate values significantly different ($P<0.05$, ANOVA followed by Tukey test).

Figure 6. Subcellular localization of NRAMP6 in Arabidopsis plants.

(a and b) Representative pictures (a) and quantitative data (b) of subcellular localization of NRAMP6-YFP under the control of UBQ10 promoter in Arabidopsis roots under different Mn conditions. Roots of *pUBQ10:NRAMP6-YFP* transgenic lines with *nramp6-1nramp1* background were grown on a nutrient agar medium

containing 0 (-Mn) or 10 μM Mn (+Mn) for 7 d. The plant roots were stained with 10 μM FM4-64 for 10 min and then subjected to fluorescence observation of YFP and FM4-64. Eight cells from each of three roots were subjected to YFP intensity measurement and the ratio of the YFP signal in plasma membrane to intracellular membrane was calculated. The arrow indicates the intracellular NRAMP6-YFP. Scale bar = 100 μm. Asterisks indicate significantly different ratios (Student's *t* test, ***P<0.001).

(c)–(e) Effect of Mn deficiency on NRAMP6-HA protein accumulation (b and c) and subcellular localization (e). Eighteen-day-old seedlings of a *pUBQ10:NRAMP6-HA* transgenic line with *nramp6-1nramp1* background (c and e) or *pNRAMP6:NRAMP6-HA* transgenic lines with *nramp1* background (d) were exposed to 0 (-Mn) or 10 μM Mn (+Mn) for 9 d. Roots and shoots were then excised for the immunoblot analysis of NRAMP6-HA. (e) Analysis of NRAMP6-HA subcellular localization by aqueous two-phase partitioning. Samples from the upper (U) and lower (L) phases after partitioning were subjected to the immunoblot analysis of NRAMP6-HA, H^+-ATPase (plasma membrane marker) and BiP (ER marker).

Figure 7. NRAMP6 has Mn transport capacity in yeast.

NRAMP6 was constructed into a yeast low copy vector pYC2. The NRAMP6-pYC2 and pYC2 empty vectors were, respectively, transformed into wild-type yeast strain BY4741 and two mutant strains *Δsmf1* and *Δsmf2*. Yeast cells were grown on SD medium without uracil containing galactose in the absence or presence of 5 mM Mn-chelator EGTA. Five microliter yeasts (OD_{600}=0.6) of 10-fold serial dilutions were spotted and grown at 30 □ for 3 d.

Figure. 1

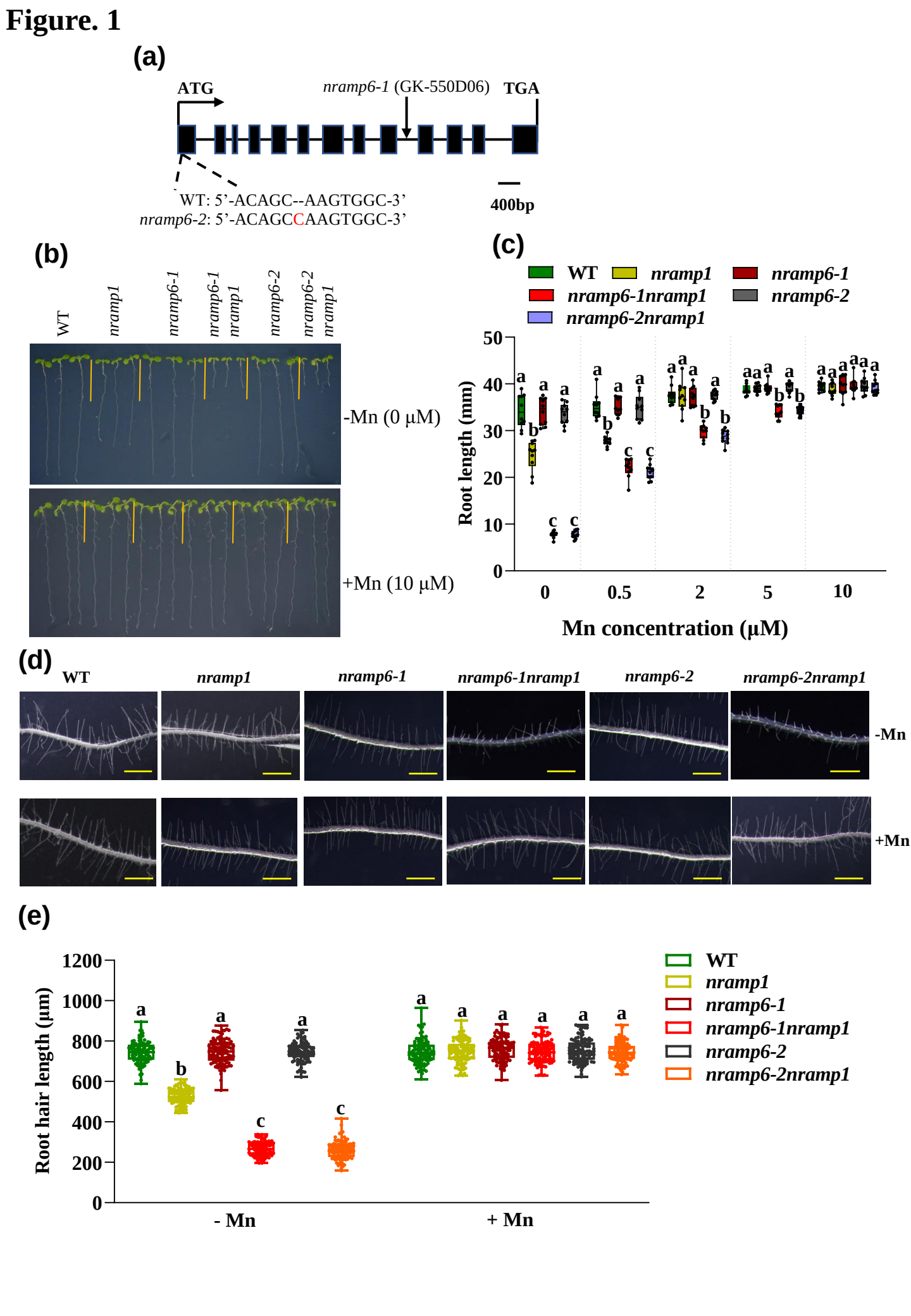
(a)
ATG
nramp6-1 (GK-550D06)
TGA
WT: 5'-ACAGC--AAGTGGC-3'
nramp6-2: 5'-ACAGCCAAGTGGC-3'
400bp
(b)
WT
nramp1
nramp6-1
nramp6-1 nramp1
nramp6-2
nramp6-2 nramp1
-Mn (0 μM)
+Mn (10 μM)
(c)
WT
nramp1
nramp6-1
nramp6-1nramp1
nramp6-2
nramp6-2nramp1
Root length (mm)
Mn concentration (μM)
(d)
WT
nramp1
nramp6-1
nramp6-1nramp1
nramp6-2
nramp6-2nramp1
-Mn
+Mn
(e)
Root hair length (μm)
- Mn
+ Mn
WT
nramp1
nramp6-1
nramp6-1nramp1
nramp6-2
nramp6-2nramp1

Figure. 2

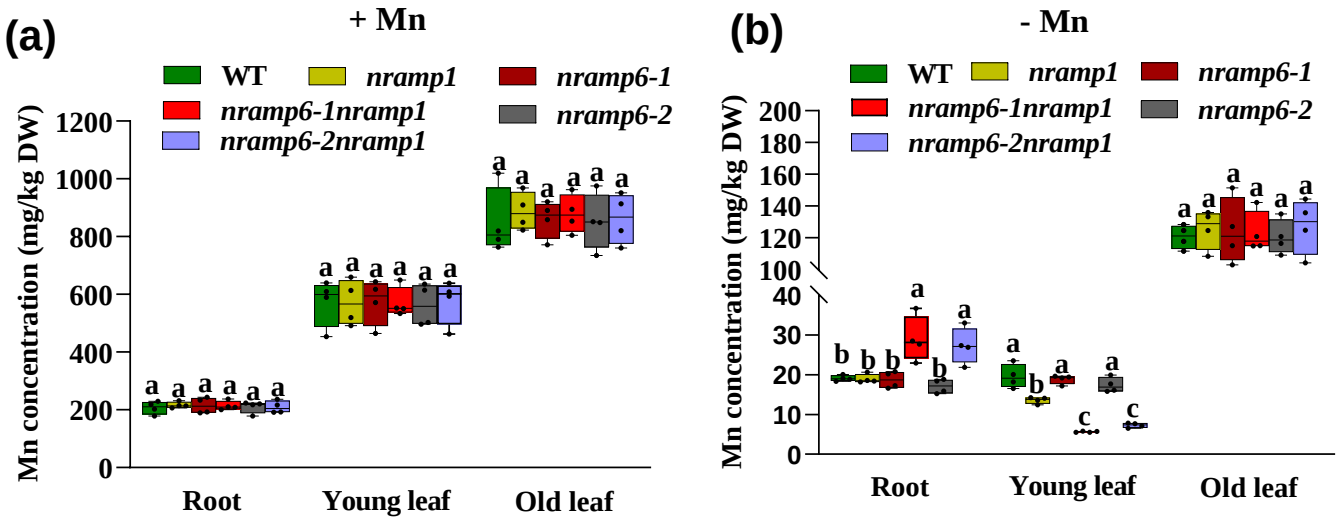
(a)
+ Mn
WT
nramp1
nramp6-1
nramp6-1nramp1
nramp6-2
nramp6-2nramp1
Mn concentration (mg/kg DW)
1200
1000
800
600
400
200
0
Root
Young leaf
Old leaf
(b)
- Mn
WT
nramp1
nramp6-1
nramp6-1nramp1
nramp6-2
nramp6-2nramp1
Mn concentration (mg/kg DW)
200
180
160
140
120
100
40
30
20
10
0
Root
Young leaf
Old leaf

Figure. 3

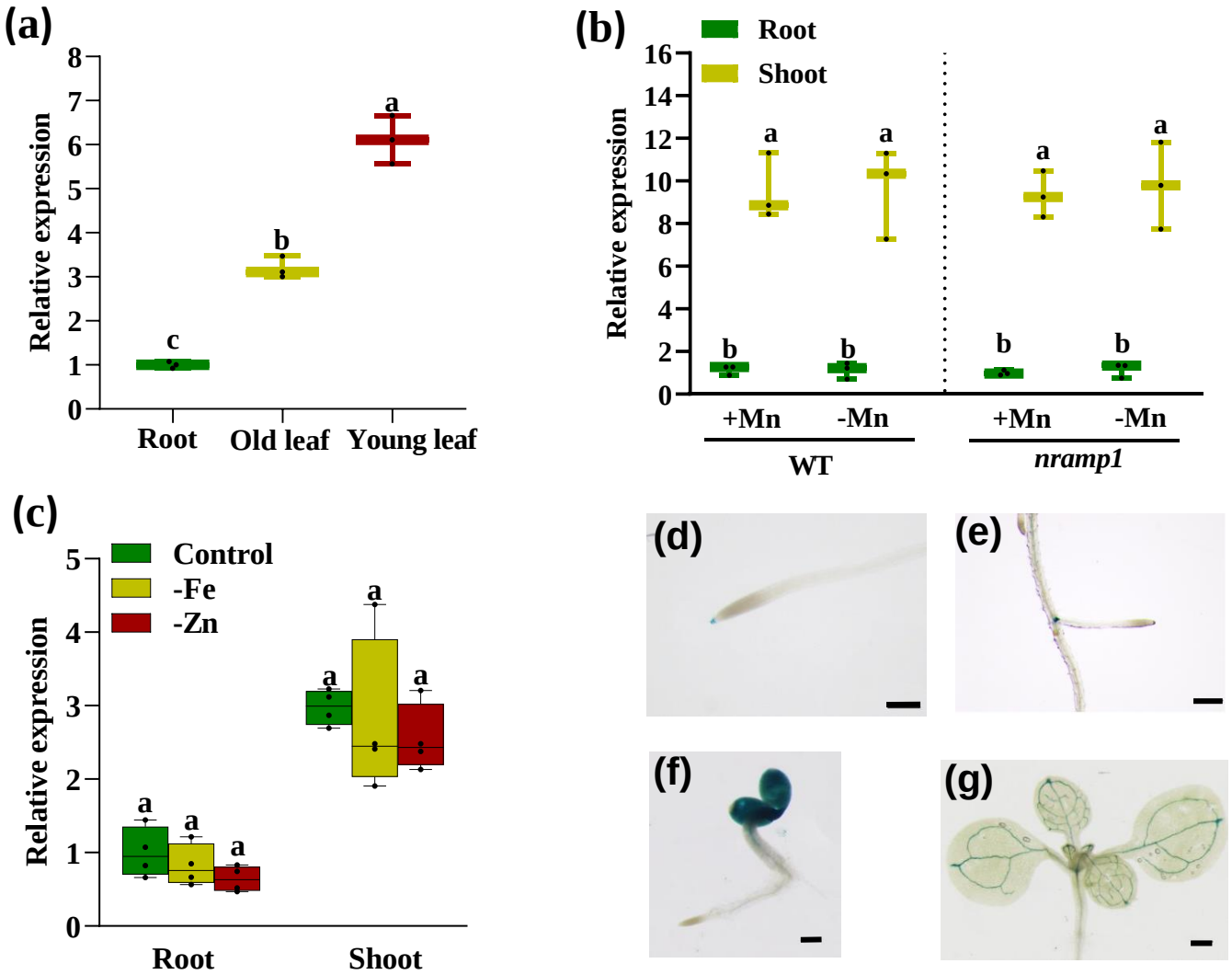
(a)
Relative expression
Root
Old leaf
Young leaf
(b)
Root
Shoot
Relative expression
+Mn
-Mn
WT
nramp1
(c)
Control
-Fe
-Zn
Relative expression
Root
Shoot
(d)
(e)
(f)
(g)

Figure. 4

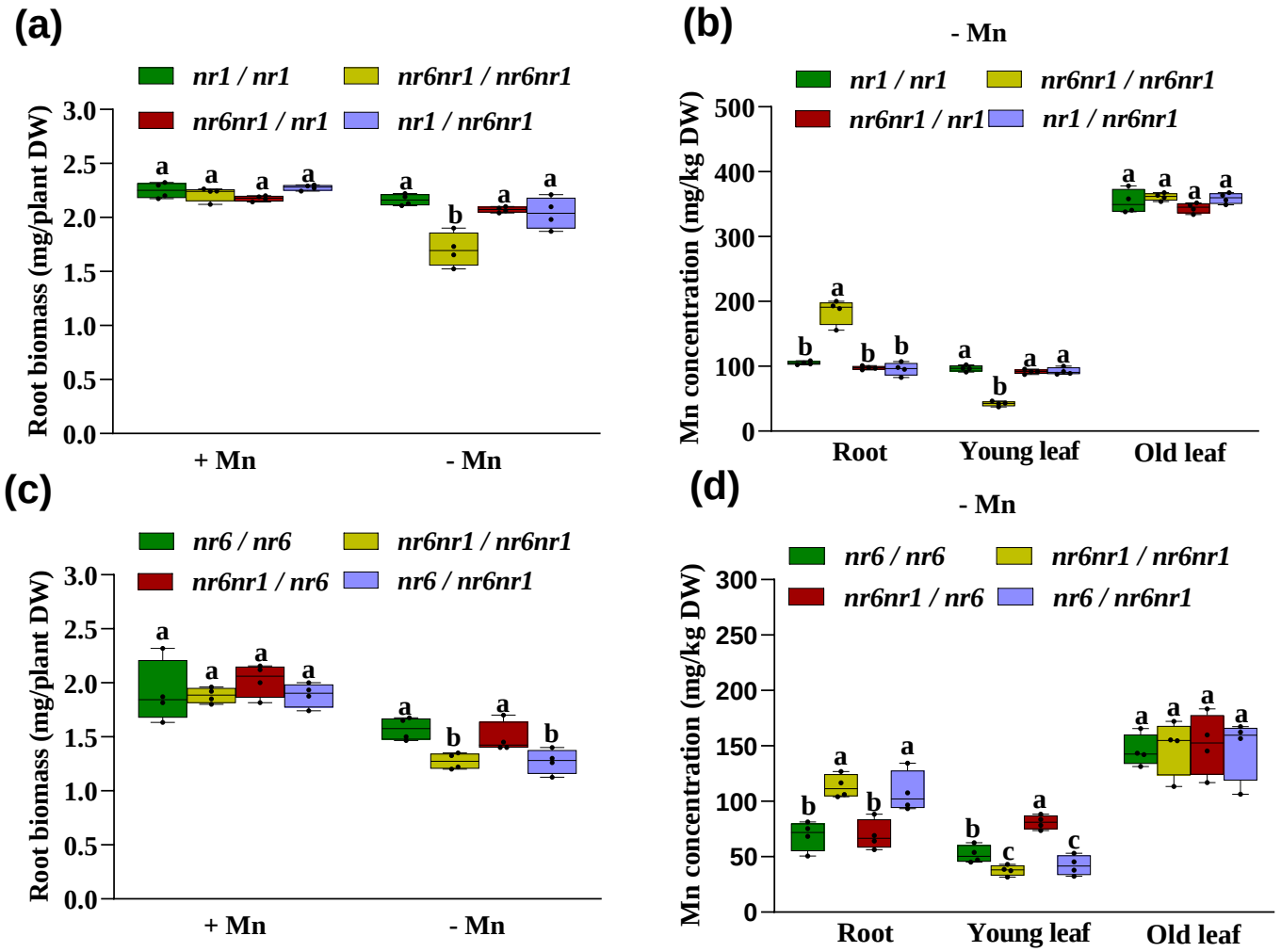
(a)
nr1 / nr1
nr6nr1 / nr6nr1
nr6nr1 / nr1
nr1 / nr6nr1
Root biomass (mg/plant DW)
3.0
2.5
2.0
1.5
1.0
0.5
0.0
a a a a
a b a a
+ Mn
- Mn
(b)
- Mn
nr1 / nr1
nr6nr1 / nr6nr1
nr6nr1 / nr1
nr1 / nr6nr1
Mn concentration (mg/kg DW)
500
400
300
200
100
0
b a b b
a b a a
a a a a
Root
Young leaf
Old leaf
(c)
nr6 / nr6
nr6nr1 / nr6nr1
nr6nr1 / nr6
nr6 / nr6nr1
Root biomass (mg/plant DW)
3.0
2.5
2.0
1.5
1.0
0.5
0.0
a a a a
a b a b
+ Mn
- Mn
(d)
- Mn
nr6 / nr6
nr6nr1 / nr6nr1
nr6nr1 / nr6
nr6 / nr6nr1
Mn concentration (mg/kg DW)
300
250
200
150
100
50
0
b a b a
b c a c
a a a a
Root
Young leaf
Old leaf

Figure. 5

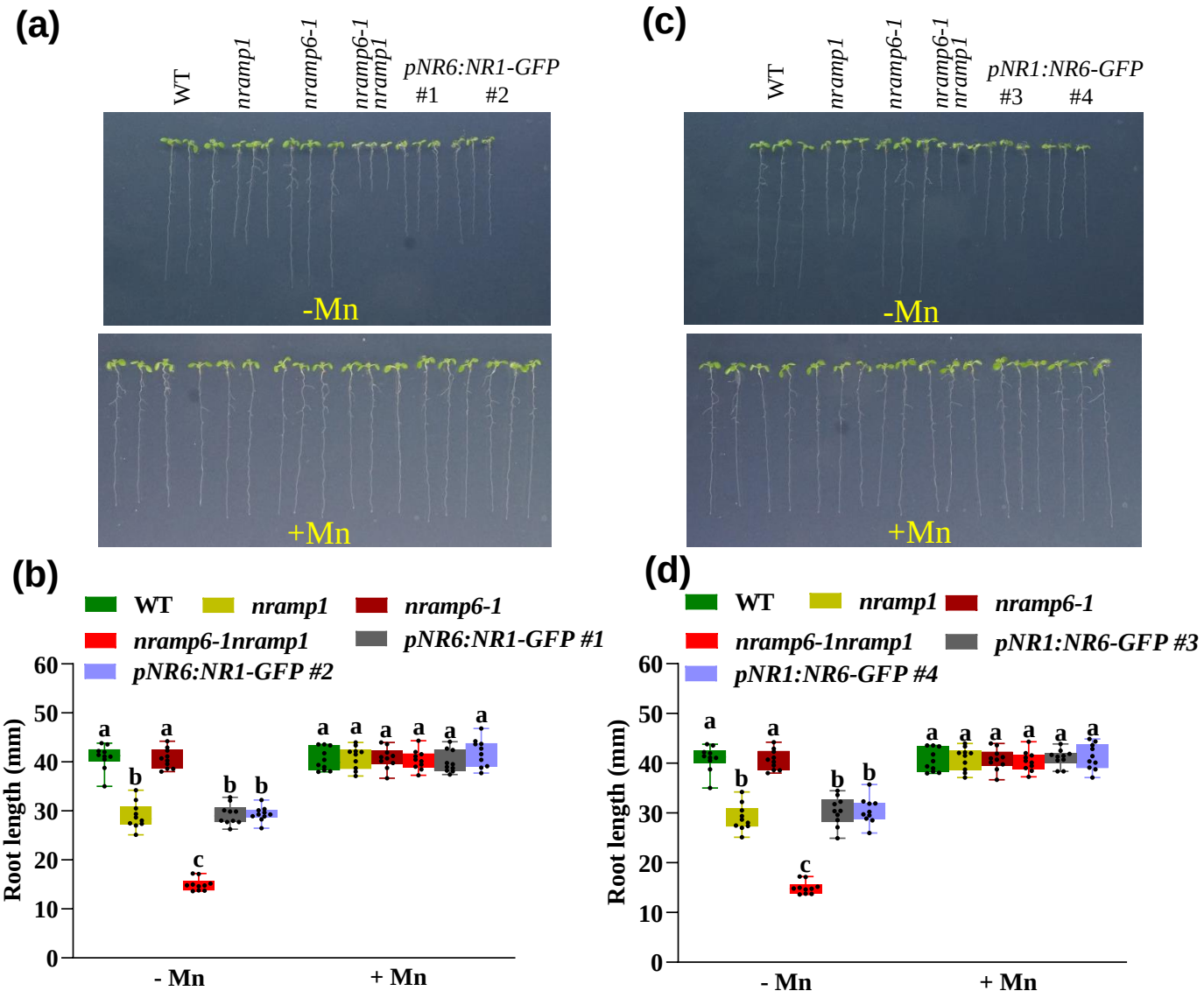
(a)
WT
nramp1
nramp6-1
nramp6-1 nramp1
pNR6:NR1-GFP #1
pNR6:NR1-GFP #2
-Mn
+Mn
(c)
WT
nramp1
nramp6-1
nramp6-1 nramp1
pNR1:NR6-GFP #3
pNR1:NR6-GFP #4
-Mn
+Mn
(b)
WT
nramp1
nramp6-1
nramp6-1nramp1
pNR6:NR1-GFP #1
pNR6:NR1-GFP #2
Root length (mm)
0
10
20
30
40
50
60
a
b
a
c
b
b
a
a
a
a
a
a
- Mn
+ Mn
(d)
WT
nramp1
nramp6-1
nramp6-1nramp1
pNR1:NR6-GFP #3
pNR1:NR6-GFP #4
Root length (mm)
0
10
20
30
40
50
60
a
b
a
c
b
b
a
a
a
a
a
a
- Mn
+ Mn

Figure. 6

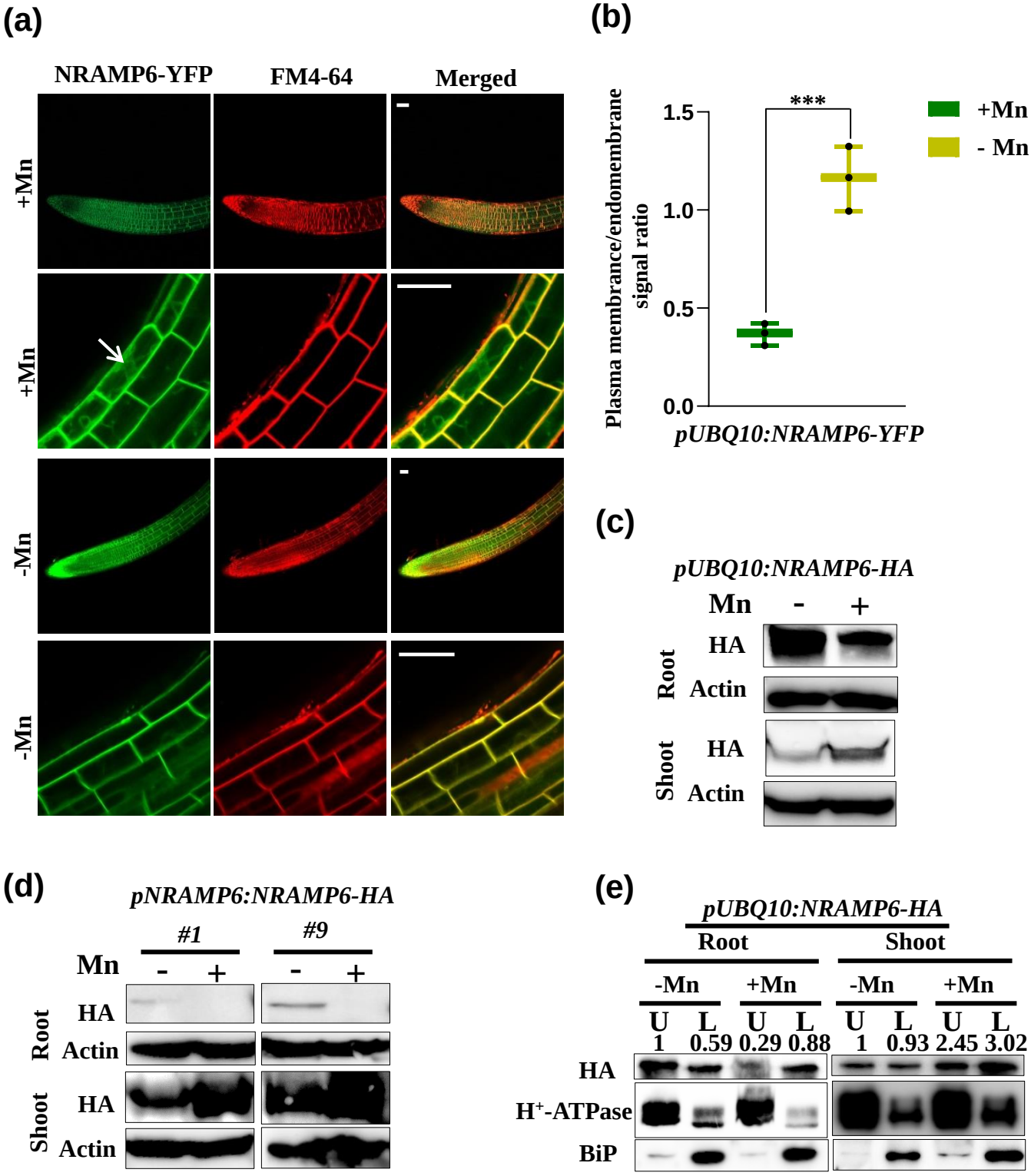
(a)
NRAMP6-YFP
FM4-64
Merged
+Mn
+Mn
-Mn
-Mn
(b)
Plasma membrance/endomembrane signal ratio
1.5
1.0
0.5
0.0
***
+Mn
- Mn
pUBQ10:NRAMP6-YFP
(c)
pUBQ10:NRAMP6-HA
Mn - +
Root
HA
Actin
Shoot
HA
Actin
(d)
pNRAMP6:NRAMP6-HA
#1
#9
Mn - + - +
Root
HA
Actin
Shoot
HA
Actin
(e)
pUBQ10:NRAMP6-HA
Root
Shoot
-Mn
+Mn
-Mn
+Mn
U L U L U L U L
1 0.59 0.29 0.88 1 0.93 2.45 3.02
HA
H+-ATPase
BiP

Figure. 7

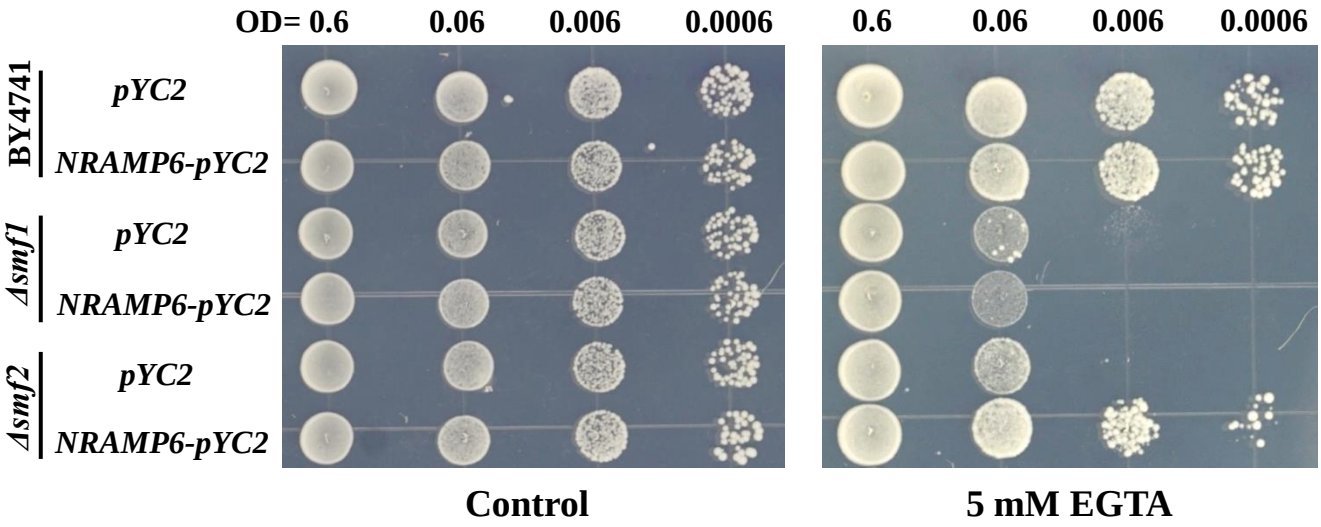
OD= 0.6
0.06
0.006
0.0006
0.6
0.06
0.006
0.0006
BY4741
pYC2
NRAMP6-pYC2
Δsmf1
pYC2
NRAMP6-pYC2
Δsmf2
pYC2
NRAMP6-pYC2
Control
5 mM EGTA